Applied Water Science (2022) 12:118
https://doi.org/10.1007/s13201-022-01628-0

ORIGINAL ARTICLE

TiO_2 and its binary $ZnTiO_2$ and ternary $CdZnTiO_2$ nanocomposites as efficient photocatalysts for the organic dyes degradation

Shakeel Khan[1] · Muhammad Sadiq[2] · Dae-sung Kim[3] · Mahboob Ullah[3] · Niaz Muhammad[1]

Received: 25 October 2021 / Accepted: 8 March 2022 / Published online: 15 April 2022

Abstract

Large band gap and high electron–hole pair recombination rate limits practical application of TiO_2 as a photocatalyst. Different methods are developed to remove or minimize the aforementioned limitations of TiO_2. In this study, TiO_2 nanoparticles were coupled with ZnO and CdO to address the above-mentioned limitations and hence to enhance the photocatalytic activity of TiO_2. TiO_2, $ZnTiO_2$ and $CdZnTiO_2$ nanocomposites were synthesized by simple co-precipitation method. The as-synthesized materials were characterized by scanning electron microscopy (SEM), transmission electron microscopy (TEM), energy-dispersive X-ray (EDX), X-ray diffraction (XRD), Brunauer–Emmett–Teller (BET) and UV–visible spectrophotometry. Morphological analysis revealed that neat TiO_2 is mostly agglomerated in spherical form. Their coupling with ZnO and CdO has increased the particle size. TEM analysis showed that $CdZnTiO_2$ is highly crystalline having uniform mixing of CdO and ZnO particles with TiO_2 in the ternary nanocomposite. The TEM images also showed that the sizes of the entire ternary $CdZnTiO_2$ nanocomposites are mostly below 50 nm. XRD analysis confirmed the anatase TiO_2, while the UV–visible analysis revealed the shifting toward higher wavelength. The band gap energy of TiO_2 (2.65 eV) was decreased to 2.64 and 2.49 eV for $ZnTiO_2$ and $CdZnTiO_2$, respectively. The photodegradation results revealed that TiO_2, $ZnTiO_2$ and $CdZnTiO_2$ degraded about 82, 90 and 94% methylene blue dye, respectively, within 120 min. Similarly, the $CdZnTiO_2$ degraded 96% methyl orange dye within 100 min. It was observed that photodegradation of the dyes increases by increasing photocatalyst dosage and pH of the medium.

Keywords TiO_2 · Nanocomposites · Photodegradation · Photocatalyst · Methylene blue · Methyl orange

Introduction

Organic dyes are the common water pollutants found in the effluents of different industries such as leather, textile, cosmetics, food and paper (Khan et al. 2019). Dyes are mostly stable synthetic compounds, resistant to sunlight, high temperatures and microbial attack (Jose et al. 2021). Most of the synthetic dyes and their metabolic intermediate products are found to be non-biodegradable, toxic, carcinogenic and mutagenic due to their large size and complex structures (Khan et al. 2020c; Ledakowicz and Paździor 2021). Therefore, developing an efficient and cost-effective method for dyes containing wastewater treatment is very essential (Khrueakham et al. 2021). Various physical, biological and chemical techniques are utilized for the removal of dyes such as adsorption (Almarri 2021; Eisazadeh et al. 2021), biodegradation (Srinivasan and Sadasivam 2021; Mohanty and Kumar 2021), nanofiltration (Hidalgo et al. 2020), electrochemical degradation (Droguett et al. 2020), ozonation (Kasiri et al. 2013), coagulation (Mohammed Redha 2020) and photocatalytic degradation. Conventional treatment methods have some associated disadvantages such as high cost, operation difficulty, environmental impact, sludge production, pre-treatment requirements, generation of toxic byproducts, lower feasibility, efficiency and reliability (Khan et al. 2020d).

Currently photo-catalysis is one of the most potential approaches for the degradation of dyes during wastewater

✉ Niaz Muhammad
drniaz@awkum.edu.pk

[1] Department of Chemistry, Abdul Wali Khan University, Mardan, Pakistan

[2] Department of Chemistry, University of Malakand, Chakdara, Dir (Lower), Pakistan

[3] Energy and Environment Division, Korea Institute of Ceramic Engineering and Technology, Jinju-si, Gyeongsangnam-do, Korea

treatment, owing to its low mammalian toxicity, high efficiency, low cost and lack of secondary pollution (Su et al. 2021; Rafiq et al. 2021) (Sonkusare et al. 2020; Gupta et al. 2020; Kumar et al. 2021; Karuppusamy et al. 2021). This technology has the ability to degrade organic pollutants into simple and non-toxic inorganic species such as CO_2 and H_2O2^1–23. Transition-metal oxides are the most promising photocatalysts for cleaning wastewater in a reliable, facile, quick and eco-friendly way (Nazim et al. 2021). Among metal oxides, TiO_2 is the most studied material owing to its abundance, non-toxicity, low cost, high photo-activity and chemical stability (Lee et al. 2020). However, large band gap and higher recombination rate of activated electron–hole pair are the main drawbacks restricting the practical applications of TiO_2 as photocatalyst (Kiwaan et al. 2020). TiO_2 modified with different materials has received extensive attention in the field of photocatalysis as modification can impart excellent chemical and physical properties, reduce band gap and decrease electron–hole pair recombination (Li et al. 2020). Various efforts were conducted in order to modify TiO_2 for enhancing its photocatalytic activity for the dyes degradation such as doping with metals (Khlyustova et al. 2020), metalloids (Niu et al. 2020), non-metal (Pillai et al. 2020), supporting on a medium such as multi-walled carbon nanotubes (MWCNTs) (Zada et al. 2020b), dye sensitization (Shang et al. 2011) and to form binary (Dontsova et al. 2020) and ternary nanocomposites (Shehzad et al. 2020).

In the present work, the photocatalytic efficiency of TiO_2 was enhanced by coupling with cadmium and zinc to form binary $ZnTiO_2$ and ternary $CdZnTiO_2$ nanocomposites through co-precipitation method. The synthesized materials were characterized via scanning electron microscopy (SEM), transmission electron microscopy (TEM), energy-dispersive X-ray (EDX), X-ray diffraction (XRD), Brunauer–Emmett–Teller (BET) and UV–visible spectrophotometry. The as-synthesized neat TiO_2, $ZnTiO_2$ and $CdZnTiO_2$ were utilized for the photocatalytic degradation of methylene blue (MB) and methyl orange (MO) dyes in aqueous medium under UV-light irradiation. MB is a recalcitrant organic pollutant with mutagenic and cariogenic nature. It causes several health issues such as skin irritation, eye burns, vomiting and nausea to humans (Radoor et al. 2021). Similarly, MO is highly toxic and can cause vomiting, shock, increased heart rate, quadriplegia, cyanosis, jaundice and tissue necrosis in humans (Khan et al. 2020b). The effect of irradiation time, pH of the medium and catalyst dosage on photodegradation efficiency was investigated.

Experimental work

Materials

Cadmium(II) chloride pentahydrate [$CdCl_2.5H_2O$], zinc(II) acetate dihydrate [$Zn(CH_3COO)_2.2H_2O$] and titanium(IV) isopropoxide [$C_{12}H_{28}O_4Ti$] were purchased from BDH. Analytical grade sodium hydroxide, methylene blue and methyl orange were purchased from Sigma–Aldrich.

Synthesis of TiO_2 nanoparticles

TiO_2 nanoparticles were synthesized by precipitation method using titanium(IV) isopropoxide and deionized water. Five milliliters of titanium(IV) isopropoxide was added to 8 mL of deionized water at 45 °C. The mixture was stirred continuously for 1 h, and as a result, a white precipitate was obtained in the beaker. The precipitate was centrifuged, filtered and washed several times with deionized water and methanol in order to remove the undesired materials. The obtained powder was dried in an oven at 80 °C for 8 h and further annealed at 450 °C for 5 h.

Synthesis of $ZnTiO_2$ nanocomposite

$ZnTiO_2$ nanocomposite was prepared by co-precipitation method. Zinc(II) acetate dihydrate and titanium(IV) isopropoxide were used as zinc and titanium precursors, respectively. In the first step, zinc(II) acetate dihydrate (0.049 mol, 10.8 g) was added to 250 mL deionized water and kept under stirring at room temperature for 30 min. Then, 1 M NaOH was added dropwise to adjust the pH 9–10. During this process, a white precipitate of $Zn(OH)_2$ was slowly formed and subsequently settled down when kept undisturbed for 10 min. The precipitate was collected via centrifugation and washed with deionized water and methanol several times to remove residual reactants. Finally, the precipitate was dried in an oven at 80 °C for 5 h and further annealed at 500 °C for 4 h to get ZnO nanoparticles in powdered form. In the second step, the synthesized ZnO nanoparticles (0.01 mol) were dispersed in 5 mL of aqueous methanol using a sonicator for 30 min. Subsequently, the ZnO dispersion was introduced into the TiO_2 (0.39 mol) dispersion in 5 mL aqueous methanol to achieve bimetallic $ZnTiO_2$ nanocomposite. The solution was continuously stirred at 80 °C for 30 min, and the precipitates were collected by centrifugation. The final product was aged overnight and dried at 100 °C for 2 h.

Synthesis of $CdZnTiO_2$ nanocomposite

Ternary $CdZnTiO_2$ nanocomposite was prepared by co-precipitation method. Zinc(II) acetate dihydrate, cadmium(II) chloride pentahydrate and titanium(IV) isopropoxide were used as zinc, cadmium and titanium precursors, respectively. In the first step, zinc(II) acetate dihydrate (0.025 mol, 5.48 g) and cadmium(II) chloride pentahydrate (0.025 mol, 6.84 g) were separately dissolved in 250 mL deionized water and kept under stirring at room temperature for 30 min. Then, to these well-mixed solutions, 1 M NaOH was added dropwise

to adjust the pH 9–10. During this process, the precipitates were slowly formed in each beaker. The precipitates were then collected by centrifugation and sequentially washed with deionized water and methanol several times to remove residual reactants. The precipitates were then dried in an oven at 80 °C for 5 h and further annealed at 500 °C for 4 h. The synthesized CdO (0.001 M) and ZnO (0.01 M) nanoparticles were separately dispersed in 5 mL of aqueous methanol using a sonicator for 30 min. Subsequently, the CdO and ZnO dispersions were introduced into the TiO_2 solution (1 M) in aqueous methanol to achieve ternary $ZnCdTiO_2$ nanocomposites. The solutions were continuously sonicated at 80 °C for 30 min, and the precipitates were collected by centrifugation. The final product was aged overnight and dried at 100 °C for 3 h.

Characterization

The morphology of the synthesized photocatalysts was investigated by SEM (model no. JEOL-5910, Japan). The EDX analysis was performed by EDX (model INCA 200/Oxford Instrument, UK), while the phase and crystallite size were scrutinized by XRD measurement (model JEOL-300). The particles size and shape of the ternary nanocomposite were investigated with TEM (Tecnai F-20 FEI, USA). The Brunauer–Emmett–Teller (BET) surface area and the porosity of the samples were studied using a nitrogen adsorption instrument (Micromeritics ASAP 2020). The photodegradation study of MB and MO dyes was monitored by using a UV–Vis spectrophotometer (UV-1800, Shimadzu, Japan).

Photodegradation of the dyes

TiO_2, $ZnTiO_2$ and $CdZnTiO_2$ (0.02 g) were added separately to 5 mL deionized water and sonicated for 30 min. After sonication, 10 mL of the dye solution (30 ppm) was added to each beaker and sealed with colorless plastic to allow light penetration and to avoid dehydration. The mixtures were kept in dark for 30 min in order to establish adsorption–desorption equilibrium. The solution mixtures were then placed under UV light (254 nm, 15 W) with constant stirring for a given specific UV irradiation time. After irradiation, the catalyst was separated from the dye solution by centrifugation (1200 rpm, 10 min). The photodegradation study was monitored by a UV–Vis spectrophotometer. The %degradation of the dyes in aqueous media was calculated by the following equation:

$$\text{Degradation rate } (\%) = \left(\frac{A_o - A}{A_o}\right) \times 100$$

where A_o is the initial absorbance of the dye and A is the dye absorbance after UV irradiation.

Results and discussion

Morphological and elemental composition study

The catalytic activity of nanoparticles depends upon their size and surface morphology. Figure 1a–i displays the SEM images of TiO_2, $ZnTiO_2$ and $CdZnTiO_2$. Figure 1a–c shows that the TiO_2 NPs are mostly spherical in agglomerated form. Figure 1d–f represents that $ZnTiO_2$ is present in spherical form and the ZnO NPs are well distributed over the TiO_2. The particles are in different sizes, and it was observed that $ZnTiO_2$ is less agglomerated as compared to neat TiO_2. The $CdZnTiO_2$ is mostly present in dispersed form, and all the particles are well mixed in the ternary nanocomposite as observed in Fig. 1g–i. The crystal structure and morphology of $CdZnTiO_2$ ternary nanocomposite were further examined through TEM analysis. Figure 2 shows the TEM images of ternary nanocomposite at different magnifications. The TEM images strongly support the results of SEM analysis. TEM images show that the ternary $CdZnTiO_2$ nanocomposites are highly crystalline with spherical geometry and mostly having size below 50 nm. Highly magnified images show that all the CdO and ZnO particles are uniformly mixed with TiO_2 in the ternary nanocomposites. The elemental compositions/purities of the synthesized samples were determined through EDX analysis. Figure 3a–c represents the EDX spectra of TiO_2, $ZnTiO_2$ and $CdZnTiO_2$, respectively, along with %atomic composition of the constituent elements, reflecting purity of the samples. The presence of Pt peaks in the EDX spectra is due to platinum spraying on sample before analysis for improving the samples imaging. The EDX spectra verify that Ti and O are the major elements, while Zn and Cd are present in minute quantities.

XRD and BET analyses

The XRD analysis was performed to examine the crystalline phase and purity. Figure 4a represents the XRD pattern of TiO_2, $ZnTiO_2$ and $CdZnTiO_2$. All the major peaks observed in the XRD pattern of TiO_2, $ZnTiO_2$ and $CdZnTiO_2$ can be indexed to the (101), (004), (200), (105), (211), (204) and (116) crystal planes of TiO_2. All the major diffraction peaks observed are well defined and can be perfectly assigned to the anatase phase TiO_2 (JCPDS-21-1272). The diffraction peak located at 36.3° can be indexed to the hexagonal wurtzite phase of ZnO. A small peak at 38.3° corresponding to the (200) planes can be indexed to a cubic pattern of CdO.

The optimal porosity and high surface area are the two essential parameters for the efficient photocatalytic

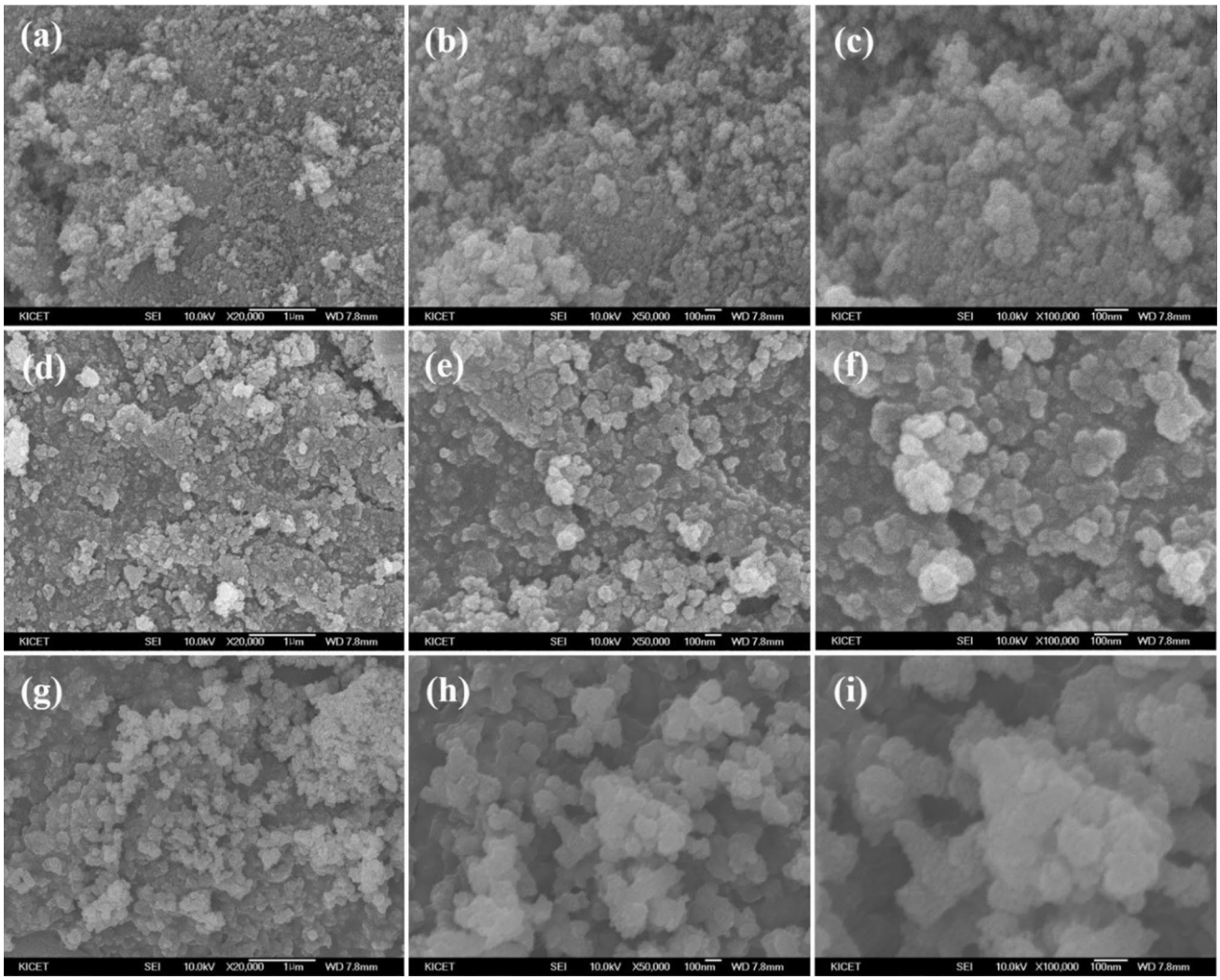

Fig. 1 SEM images of (**a**–**c**) TiO_2, (**d**–**f**) $ZnTiO_2$ and (**g**–**i**) $CdZnTiO_2$

activity of nanocomposites. Figure 4b represents the BET and adsorption–desorption plot for the ternary $CdZnTiO_2$ nanocomposite. The adsorption–desorption of nitrogen is very important to investigate the surface area, average pore size and pore volume of the synthesized materials. From the BET study and N_2 adsorption–desorption measurement, it was observed that the ternary $CdZnTiO_2$ nanocomposite exhibits type IV isotherm with a sharp increase of the adsorbed volume starting from $P/P_0 = 0.7$. This result confirms the presence of well-developed mesoporous nano-sized nature of the synthesized nanocomposite. As the relative pressure approaches 1, the shifting of the hysteresis loop to the higher indicates the presence of the microporous particles. The surface parameters such as BET surface area, pore volume and pore size of $ZnCdTiO_2$ nanocomposite are represented in Table 1.

UV–visible analysis

In order to further characterize the TiO_2 and its nanocomposites, UV–visible analysis was also performed. Figure 5 represents the UV–visible spectra of TiO_2, $ZnTiO_2$ and $CdZnTiO_2$. Figure 5 displays the UV–visible absorption spectra of TiO_2, $ZnTiO_2$ and $CdZnTiO_2$. The UV–visible absorption spectra of TiO_2 exhibit absorbance peak at 265 nm. The absorbance wavelength of $ZnTiO_2$ and $CdZnTiO_2$ was shifted toward higher wavelengths. Thus, these nanocomposites can show efficient photocatalytic activity than TiO_2.

Figure 6a–c represents Tauc plots: $(\alpha\ hv)^2$ versus energy of TiO_2, $ZnTiO_2$ and $CdZnTiO_2$, respectively. The absorption power of pure TiO_2 NPs is in blueshift. The amorphous or semicrystalline materials show a wide range of absorption

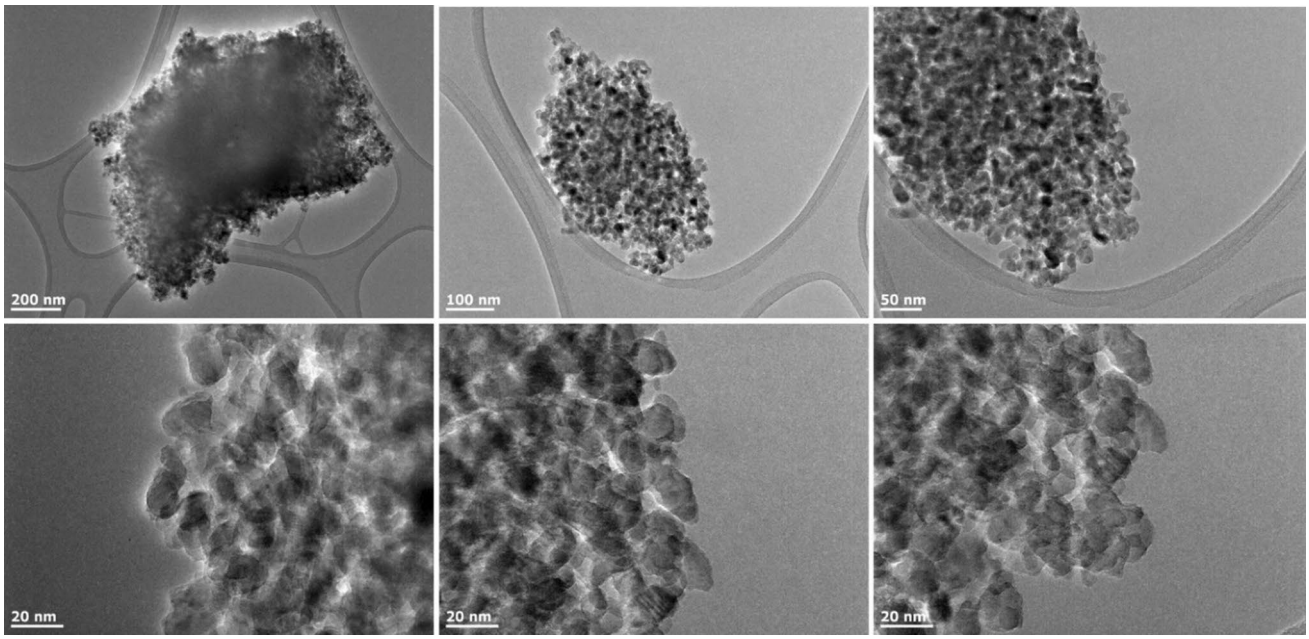

Fig. 2 TEM images of $CdZnTiO_2$

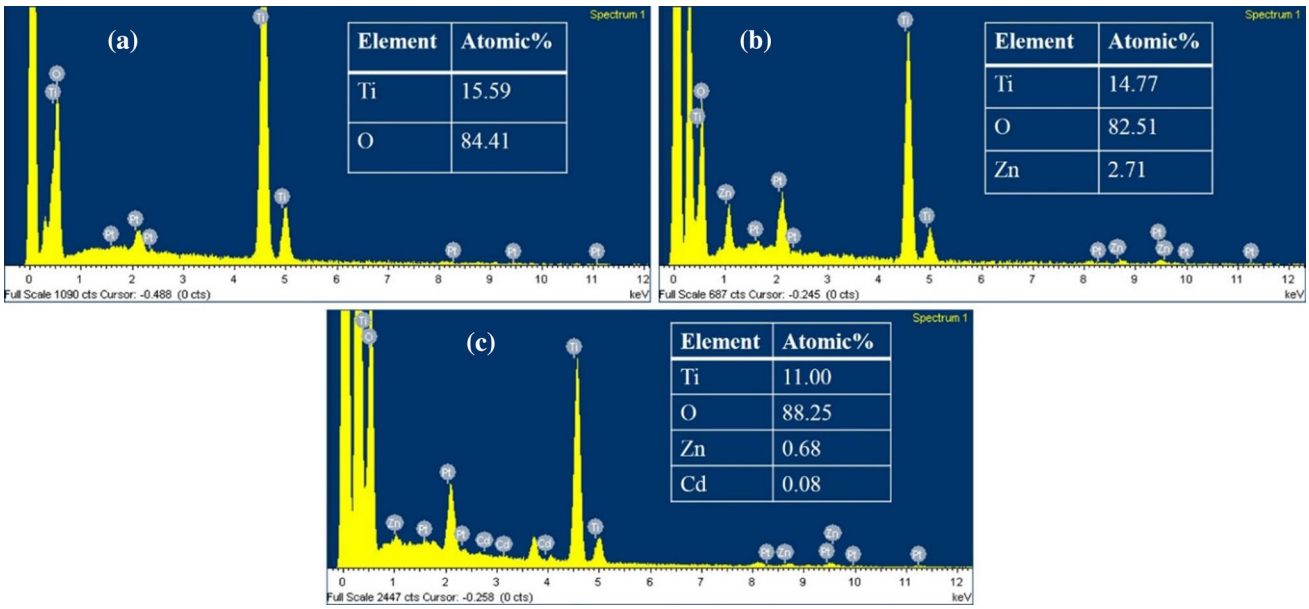

Fig. 3 EDX spectra of **a** TiO_2, **b** $ZnTiO_2$ and **c** $CdZnTiO_2$

edges, while crystallite materials have a sharp absorption edge. The band gap of synthesized materials was calculated by using Tauc plots, which show connection between the absorption edge of the sample and the energy of incident photon.

$$\alpha.\mathrm{h}.v = \mathrm{A}\left(\mathrm{h}.\mathrm{v} - E_{\mathrm{g}}\right)^{n}$$

where α = absorbance value attained from the spectra, h = Planck's constant, $v = c/\lambda$, v = frequency of the incident wave, c = velocity of light, λ = wavelength acquired from the spectra, A = constant, Eg = energy gap between the valence and conduction bands and n = parameter associated with the electronic transition and is ½ in the present case. The results clearly indicate that the band gap calculated for TiO_2 is 2.65 eV which decreased to 2.64 eV and 2.49 eV

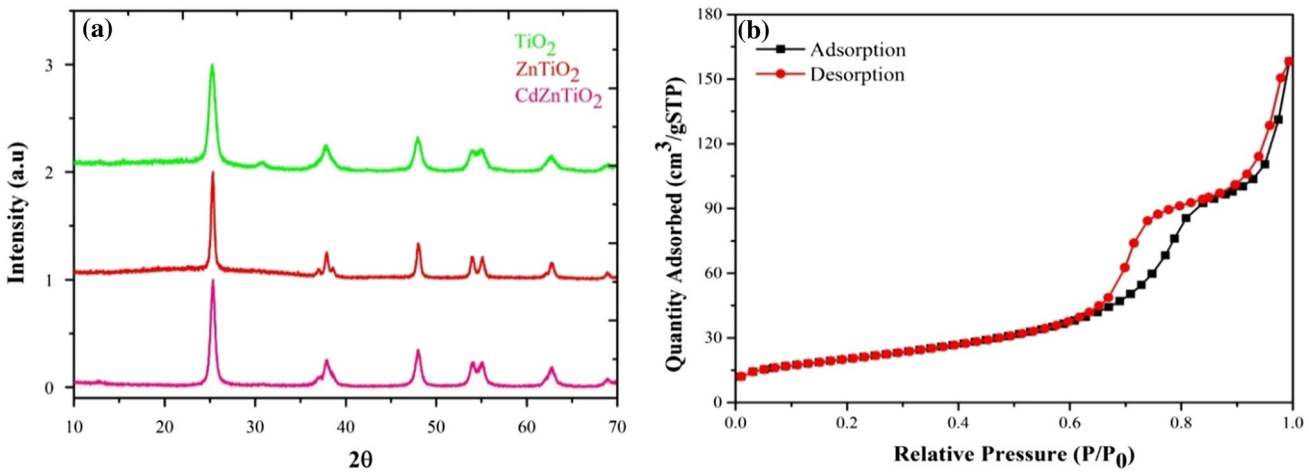

Fig. 4 **a** XRD spectra of TiO_2, $ZnTiO_2$ and $CdZnTiO_2$, **b** BET and adsorption desorption plot for $CdZnTiO_2$

Table 1 The specific surface area, pore volume and pore size of $ZnCdTiO_2$ nanocomposite

BET (m^2/g)	Pore volume (cm^3/g)	Pore size (nm)
72.7	0.2	13.4

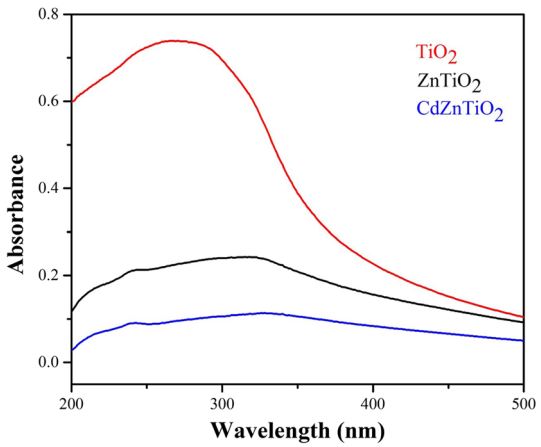

Fig. 5 UV–visible absorption spectra of TiO_2 NPs, $ZnTiO_2$ and $CdZnTiO_2$

for $ZnTiO_2$ and $CdZnTiO_2$, respectively. Figure 6d represents the optical band gap variation of TiO_2, $ZnTiO_2$ and $CdZnTiO_2$. The optical band gap decreases by coupling TiO_2 with other metal nanoparticles.

Photodegradation of methylene blue (MB) dye

The photocatalytic activity of all materials (TiO_2, $ZnTiO_2$ and $CdZnTiO_2$) was tested for the photodegradation of MB dye in aqueous medium under UV-light irradiation. Figure 7 represents the photocatalytic degradation of MB dye by TiO_2, $ZnTiO_2$ and $CdZnTiO_2$. Figure 7a–c shows the UV–visible spectra of MB dye before and after reaction under different UV-light irradiation times in the presence of TiO_2, $CdTiO_2$ and $ZnCdTiO_2$, respectively, in aqueous medium. The photodegradation efficiency of TiO_2, $CdTiO_2$ and $ZnCdTiO_2$ against MB dye was measured from the relative intensity peak of MB which gives maximum absorbance at 654 nm. This intensity of the peak decreases continuously with the increase in irradiation time. The %degradation of MB dye photodegraded by TiO_2, $CdTiO_2$ and $ZnCdTiO_2$ is presented in Fig. 7d. The photodegradation results revealed that within the maximum irradiation time of 120 min, the TiO_2, $CdTiO_2$ and $ZnCdTiO_2$ photocatalytically degraded about 82, 90 and 94% MB dye, respectively. The enhanced photodegradation of MB dye by the binary and ternary nanocomposite is due to the synergistic effect of TiO_2, ZnO and CdO.

Effect of pH of the medium

pH is the most important parameter in photodegradation of dyes as it plays an important role in generating hydroxyl radicals required for the dye degradation (Zada et al. 2020a). The effect of pH was evaluated by degrading MB dye at different pH values (2, 4, 6, 8 and 10) values, keeping photocatalyst dosage (0.02 g) and irradiation time (30 min) constant. Figure 8a–c represents the UV–visible spectra of MB dye before and after UV-light irradiation at different pH values in the presence of TiO_2, $CdTiO_2$ and $ZnCdTiO_2$, respectively. Figure 8d represents the %degradation of MB dye at different pH values in the presence of TiO_2, $CdTiO_2$ and $ZnCdTiO_2$. The %degradation results represent that about 85, 88 and 90% MB dye is degraded at pH 10 by TiO_2, $CdTiO_2$ and $ZnCdTiO_2$, respectively. The results showed

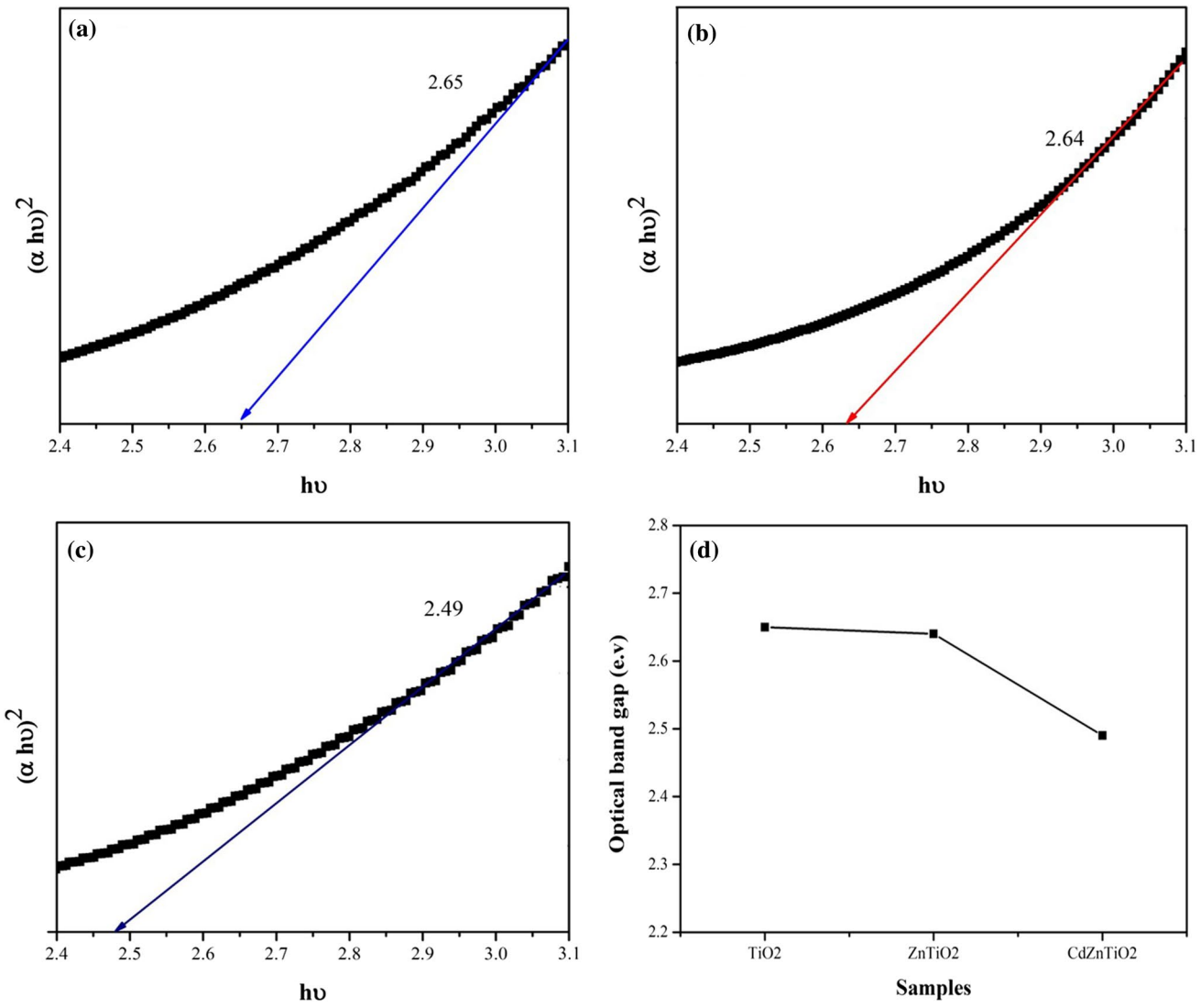

Fig. 6 Tauc plots: $(\alpha\ h\nu)^2$ versus energy for the **a** TiO_2, **b** $ZnTiO_2$, **c** $CdZnTiO_2$, **d** optical band gap variation of TiO_2 and $ZnTiO_2$, $CdZnTiO_2$

that as pH of the medium increases, photodegradation of MB dye also increases and maximum dye degradation is achieved in the basic medium. The higher photodegradation rate in the basic medium might be due to the enhanced formation of hydroxyl radicals, which are responsible for the higher degradation (Saeed et al. 2018).

Effect of photocatalysts dosage

Dyes photodegradation occurs in the active sites after adsorption on the surface of the photocatalyst, and therefore, increasing or decreasing the photocatalyst amount may affect the rate of dye degradation (Khan et al. 2020a). The effect of photocatalyst dosage on dye degradation efficiency was evaluated by applying different photocatalyst amounts keeping irradiation time (30 min) constant. Figure 9 represents the comparison of %degradation of MB dye photodegraded by different dosages of TiO_2, $CdTiO_2$ and $ZnCdTiO_2$. The results show that 0.020 g of TiO_2, $CdTiO_2$ and $ZnCdTiO_2$ degraded about 68, 72 and 81% dye, while increasing the dosage to 0.030 g, the %degradation increased to 84, 91.5 and 94.5% of the dye, respectively. The results revealed that the photodegradation of MB increases in a regular pattern by increasing photocatalyst dosage up to 0.030 g and beyond this amount no significant enhancement was observed in the photodegradation of dyes. An increase in the photocatalyst dosage beyond the optimum limit results in agglomeration of the photocatalyst particles, which decreases the particle surface area and hence photon absorption (Khan et al. 2020d).

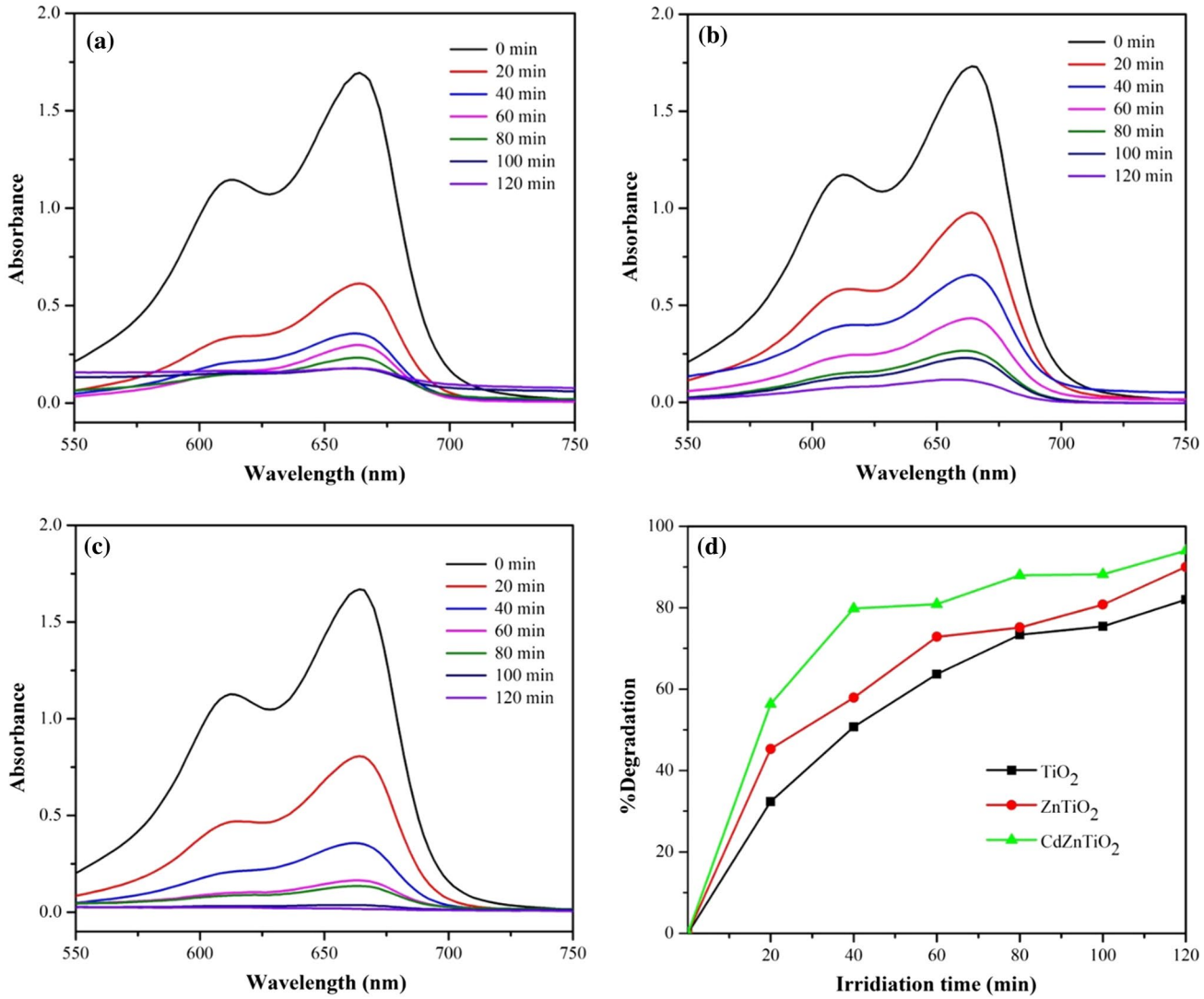

Fig. 7 **a** UV–visible absorption spectra of MB degraded by (**a**) TiO_2, **b** $ZnTiO_2$, **c** $CdZnTiO_2$, **d** comparison of % degradation of MB dye by TiO_2, $ZnTiO_2$ and $CdZnTiO_2$

Photodegradation of methyl orange (MO) dye

The ternary nanocomposite $CdZnTiO_2$ was found the most effective photocatalyst in degrading MB dye so was also employed for the photodegradation of methyl orange dye (30 ppm). Figure 10a shows the %degradation of MO dye photocatalytically degraded by $CdZnTiO_2$. The graph represents that dye degradation increases with increasing irradiation time. It was observed that the $ZnCdTiO_2$ degraded about 47% within first 20 min which increases effectively up to 96% by increasing irradiation times to 100 min. Figure 10b represents the %degradation of MO dye photodegraded (irradiation time 20 min) at different pH values in the presence of $CdZnTiO_2$ catalyst (0.02 g). The graph displays that the dye degradation efficiency increases with increasing pH of the medium. It was observed that at pH 2 only 21% dye was degraded which increased to 85.2% by increasing pH of the medium to 10. Figure 10c represents the %degradation of MO dye photodegradation by different dosages of $CdZnTiO_2$ keeping irradiation time (20 min) constant. The graph shows that MO dye degradation efficiency increases in regular pattern by increasing photocatalyst dosage. The results verified that 0.010 g of $CdZnTiO_2$ degraded about 40% dye, while 0.030 g (maximum dosage) degraded about 86.5% dye.

Photodegradation proposed mechanism

The valence band (VB) electrons (e^-) of the catalyst are excited to the conduction band (CB) by the UV light creating positive holes (h^+) in the VB. The holes react with H_2O molecules and produce hydroxyl radicals ($^{\cdot}OH$), while the electrons react with oxygen molecules and produce superoxide

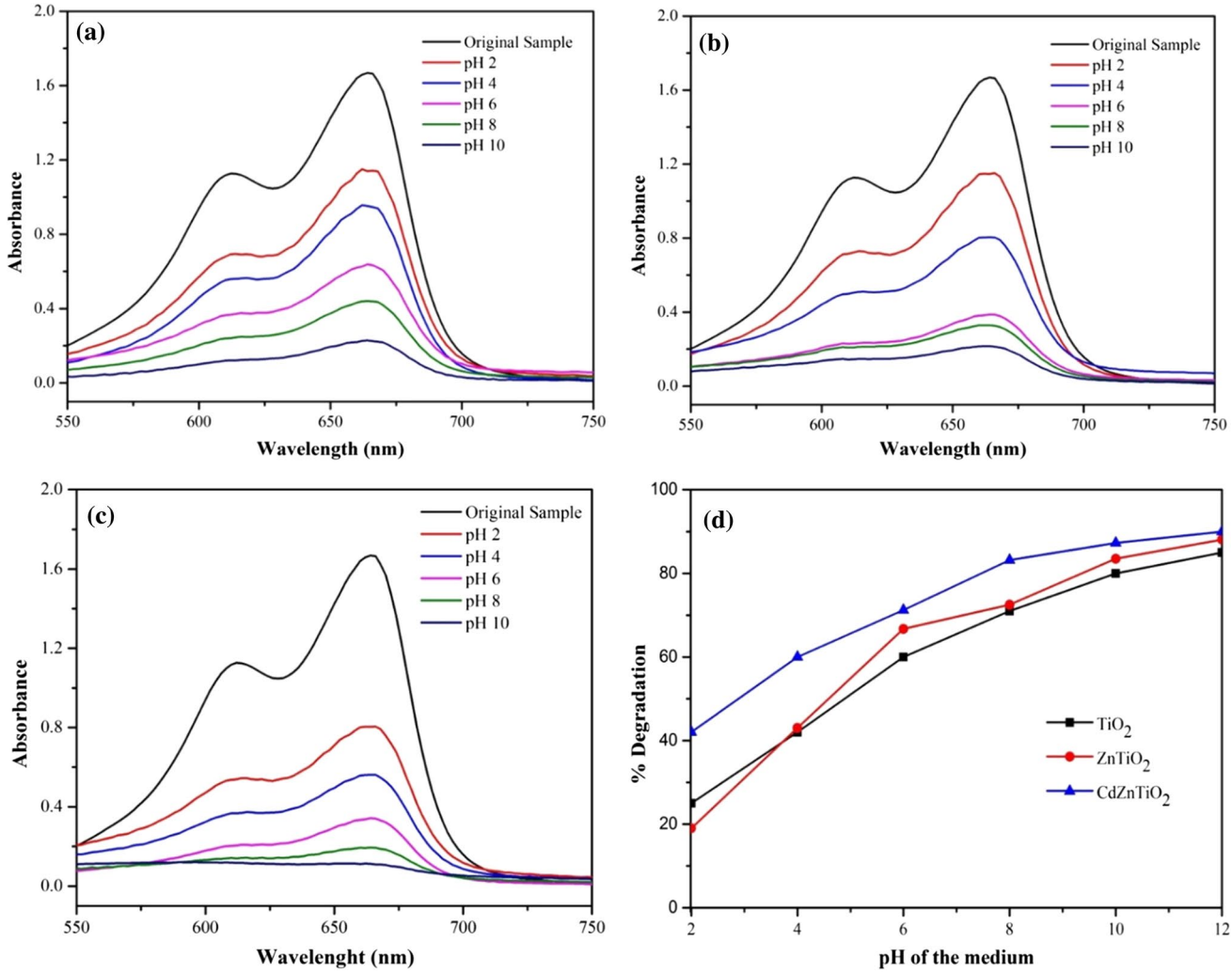

Fig. 8 UV–visible spectra of MB dye photodegraded at different pH values in the presence of **a** TiO_2, **b** $CdTiO_2$, **c** $ZnCdTiO_2$, **d** %degradation comparison of MB dye photodegraded at different pH values in the presence of TiO_2, $CdTiO_2$ and $ZnCdTiO_2$

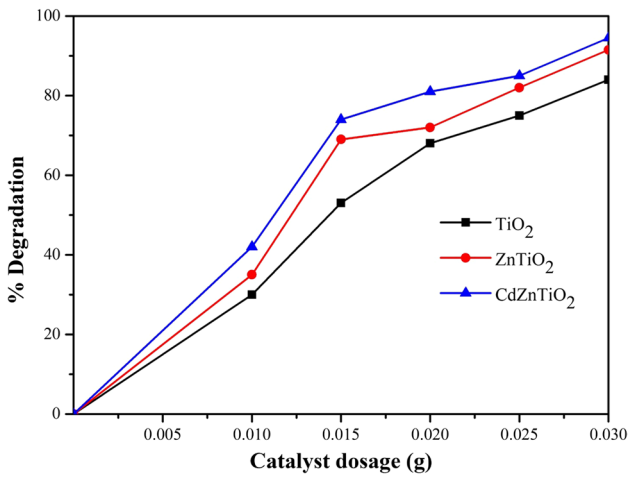

Fig. 9 Comparison of %degradation of MB dye photodegraded by different dosages of TiO_2, $ZnTiO_2$ and $CdZnTiO_2$

anion radicals ($^{\cdot}O_2^-$). These generated radicals are highly reactive and degrade dye molecules into simpler species such as H_2O and CO_2. In case of neat TiO_2, most of the generated electron–hole pairs recombine and thus the photocatalyst becomes less active. However, in case of nanocomposites the electrons present in the VB are captured by the coupled Zn and Cd. This electron capturing by coupled Zn and Cd decreases the electron–hole pair recombination rate, thus making the binary ($ZnTiO_2$) and ternary ($CdZnTiO_2$) nanocomposites more active photocatalyst. The proposed mechanism for the photodegradation of MB dye is presented in Fig. 11.

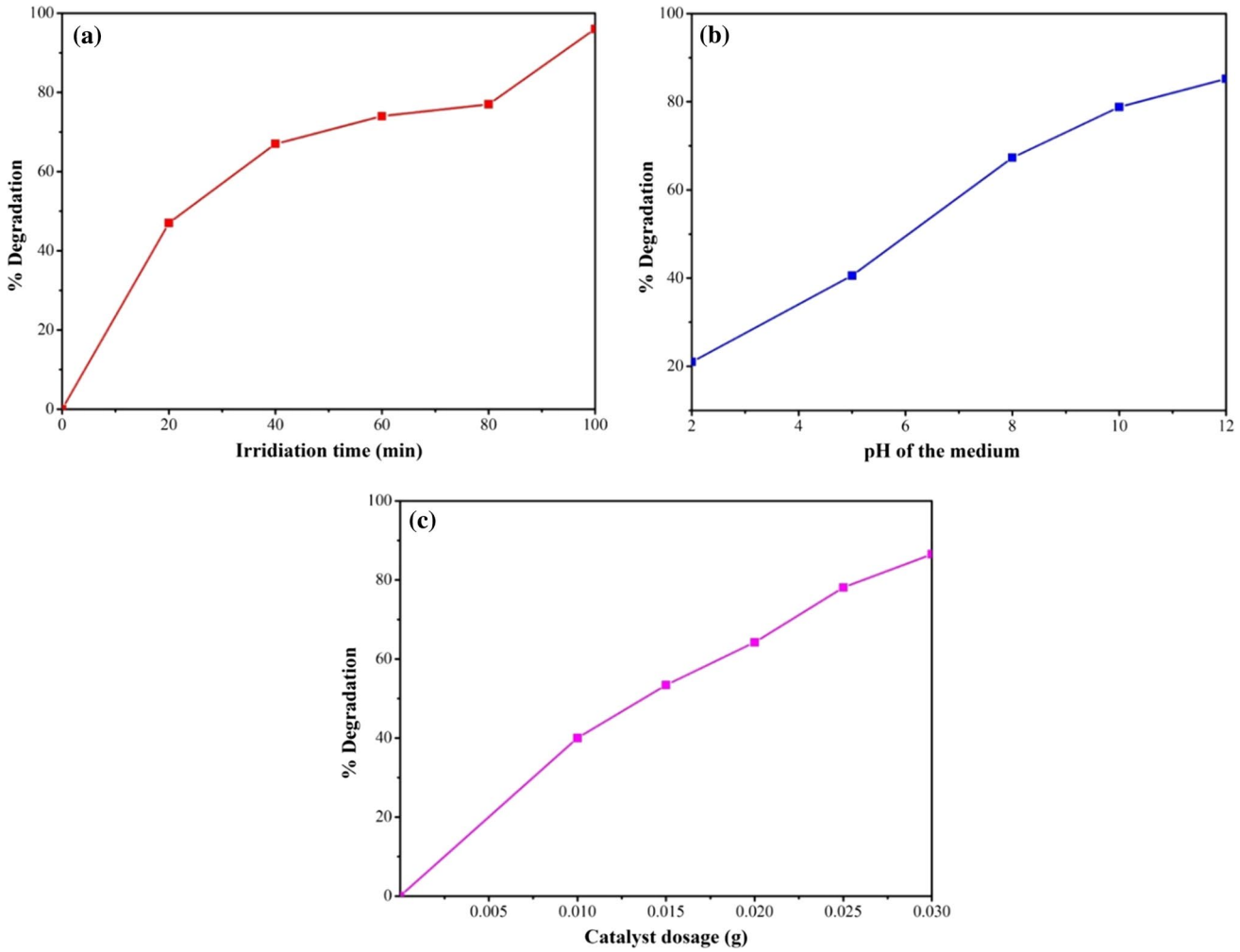

Fig. 10 %degradation of MO dye photodegraded by $CdZnTiO_2$ at **a** different irradiation times, **b** different pH values of the medium, **c** different photocatalyst dosages

Conclusion

Photocatalytic activity of TiO_2 nanoparticles was enhanced by synthesizing their binary $CdTiO_2$ and ternary $ZnCdTiO_2$ nanocomposites. Maximum photodegradation of MB was observed when the dye was irradiated by UV light for 120 min, in basic medium (pH 10) and in the presence of 0.030 g of photocatalyst. Under these optimal experimental conditions, a significant number of hydroxyl and superoxide anion radicals are generated which are responsible for the photodegradation of the dyes.

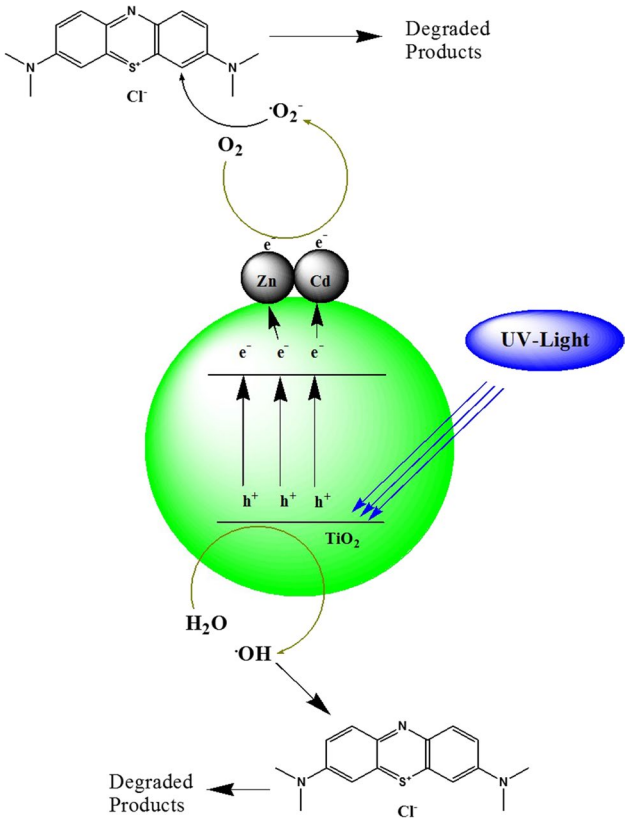

Fig. 11 Proposed mechanism for the photodegradation of MB dye by $CdZnTiO_2$

Authors' contributions All the authors contributed equally in the work.

Funding The authors received no specific funding for this work.

Declarations

Conflict of interest The authors declare that they have no known competing financial interests or personal relationships that could have appeared to influence the work reported in this paper.

References

Almarri AH (2021) Chitosan composites for thionine dye adsorption. Int J Environ Anal Chem. https://doi.org/10.1080/03067319.2021.1904915

Dontsova TA, Kutuzova AS, Bila KO et al (2020) Enhanced photocatalytic activity of TiO_2/SnO_2 binary nanocomposites. J Nanomater. https://doi.org/10.1155/2020/8349480

Droguett T, Mora-Gómez J, García-Gabaldón M et al (2020) Electrochemical degradation of reactive black 5 using two-different reactor configuration. Sci Rep 10:1–11. https://doi.org/10.1038/s41598-020-61501-5

Eisazadeh N, Eisazadeh H, Ghadakpour M (2021) Comparison between various adsorbents for direct blue dye 14 removal from aqueous solution. Fibers Polym 22:149–158. https://doi.org/10.1007/s12221-021-9885-4

Gupta NK, Ghaffari Y, Kim S et al (2020) Photocatalytic degradation of organic pollutants over MFe_2O_4 (M = Co, Ni, Cu, Zn) nanoparticles at neutral pH. Sci Rep 10:1–11. https://doi.org/10.1038/s41598-020-61930-2

Hidalgo AM, León G, Gómez M et al (2020) Removal of different dye solutions: a comparison study using a polyamide nf membrane. Membranes 10:1–16. https://doi.org/10.3390/membranes10120408

Jose A, Pai SDKR, Pinheiro D, Kasinathan K (2021) Visible light photodegradation of organic dyes using electrochemically synthesized MoO_3/ZnO. Environ Sci Pollut Res. https://doi.org/10.1007/s11356-021-14311-9

Karuppusamy I, Samuel MS, Selvarajan E et al (2021) Ultrasound-assisted synthesis of mixed calcium magnesium oxide ($CaMgO_2$) nanoflakes for photocatalytic degradation of methylene blue. J Colloid Interface Sci 584:770–778. https://doi.org/10.1016/j.jcis.2020.09.112

Kasiri MB, Modirshahla N, Mansouri H (2013) Decolorization of organic dye solution by ozonation: optimization with response surface methodology. Int J Ind Chem 4:3. https://doi.org/10.1186/2228-5547-4-3

Khan I, Sadiq M, Khan I, Saeed K (2019) Manganese dioxide nanoparticles/activated carbon composite as efficient UV and visible-light photocatalyst. Environ Sci Pollut Res 26:5140–5154. https://doi.org/10.1007/s11356-018-4055-y

Khan I, Khan AA, Khan I et al (2020a) Investigation of the photocatalytic potential enhancement of silica monolith decorated tin oxide nanoparticles through experimental and theoretical studies. New J Chem. https://doi.org/10.1039/d0nj00996b

Khan I, Khan I, Usman M et al (2020b) Nanoclay-mediated photocatalytic activity enhancement of copper oxide nanoparticles for enhanced methyl orange photodegradation. J Mater Sci Mater Electron. https://doi.org/10.1007/s10854-020-03431-6

Khan I, Khan I, Usman M et al (2020c) Nanoclay-mediated photocatalytic activity enhancement of copper oxide nanoparticles for enhanced methyl orange photodegradation. J Mater Sci Mater Electron. https://doi.org/10.1007/s10854-020-03431-6

Khan I, Saeed K, Ali N et al (2020d) Heterogeneous photodegradation of industrial dyes: an insight to different mechanisms and rate affecting parameters. J Environ Chem Eng. https://doi.org/10.1016/j.jece.2020.104364

Khlyustova A, Sirotkin N, Kusova T et al (2020) Doped TiO_2: the effect of doping elements on photocatalytic activity. Mater Adv 1:1193–1201. https://doi.org/10.1039/d0ma00171f

Khrueakham A, Masomboon J, Roongruang J, Sairiam S (2021) Efficient reactive blue 19 decolorization by the comparison of ozonation membrane contacting process and fenton oxidation. RSC Adv 11:17775–17788. https://doi.org/10.1039/d1ra01871j

Kiwaan HA, Atwee TM, Azab EA, El-Bindary AA (2020) Photocatalytic degradation of organic dyes in the presence of nanostructured titanium dioxide. J Mol Struct 1200:127115. https://doi.org/10.1016/j.molstruc.2019.127115

Kumar AP, Bilehal D, Tadesse A, Kumar D (2021) Photocatalytic degradation of organic dyes: Pd-γ-$Al_2O_3$and PdO-γ-Al_2O_3as potential photocatalysts. RSC Adv 11:6396–6406. https://doi.org/10.1039/d0ra10290c

Ledakowicz S, Paździor K (2021) Recent achievements in dyes removal focused on advanced oxidation processes integrated with biological methods. Molecules. 26(4):870

Lee SY, Kang D, Jeong S et al (2020) Photocatalytic degradation of rhodamine B Dye by TiO_2 and gold nanoparticles supported on a floating porous polydimethylsiloxane sponge under ultraviolet and visible light irradiation. ACS Omega 5:4233–4241. https://doi.org/10.1021/acsomega.9b04127

Li R, Li T, Zhou Q (2020) Impact of titanium dioxide (TiO_2) modification on its application to pollution treatment: a review. Catalysts 10:804

Mohammed Redha Z (2020) Multi-response optimization of the coagulation process of real textile wastewater using a natural coagulant. Arab J Basic Appl Sci 27:406–422. https://doi.org/10.1080/25765299.2020.1833509

Mohanty SS, Kumar A (2021) Enhanced degradation of anthraquinone dyes by microbial monoculture and developed consortium through the production of specific enzymes. Sci Rep 11:7678. https://doi.org/10.1038/s41598-021-87227-6

Nazim M, Khan AAP, Asiri AM, Kim JH (2021) Exploring rapid photocatalytic degradation of organic pollutants with porous CuO nanosheets: synthesis, dye removal, and kinetic studies at room temperature. ACS Omega 6:2601–2612. https://doi.org/10.1021/acsomega.0c04747

Niu P, Wu G, Chen P et al (2020) optimization of boron doped Tio_2 as an efficient visible light-driven photocatalyst for organic dye degradation with high reusability. Front Chem 8:172. https://doi.org/10.3389/fchem.2020.00172

Pillai VV, Lonkar SP, Alhassan SM (2020) Template-free, solid-state synthesis of hierarchically macroporous s-doped Tio_2 nano-photocatalysts for efficient water remediation. ACS Omega 5:7969–7978. https://doi.org/10.1021/acsomega.9b04409

Radoor S, Karayil J, Jayakumar A et al (2021) Release of toxic methylene blue from water by mesoporous silicalite-1: characterization, kinetics and isotherm studies. Appl Water Sci 11:110. https://doi.org/10.1007/s13201-021-01435-z

Rafiq A, Ikram M, Ali S et al (2021) Photocatalytic degradation of dyes using semiconductor photocatalysts to clean industrial water pollution. J Ind Eng Chem 97:111–128

Saeed K, Zada N, Khan I, Sadiq M (2018) Synthesis, characterization and photodegradation application of Fe-Mn and F-MWCNTs supported Fe-Mn oxides nanoparticles. Desalin Water Treat 108:362–368. https://doi.org/10.5004/dwt.2018.22010

Shang J, Zhao FW, Zhu T, Li J (2011) Photocatalytic degradation of rhodamine B by dye-sensitized TiO_2 under visible-light irradiation. Sci China Chem 54(1):167–172. https://doi.org/10.1007/s11426-010-4168-8

Shehzad N, Zafar M, Ashfaq M et al (2020) Development of $AgFeo_2$/RgO/tio_2 ternary composite photocatalysts for enhanced photocatalytic dye decolorization. Curr Comput-Aided Drug Des 10:1–15. https://doi.org/10.3390/cryst10100923

Sonkusare VN, Chaudhary RG, Bhusari GS et al (2020) Mesoporous octahedron-shaped tricobalt tetroxide nanoparticles for photocatalytic degradation of toxic dyes. ACS Omega 5:7823–7835. https://doi.org/10.1021/acsomega.9b03998

Srinivasan S, Sadasivam SK (2021) Biodegradation of textile azo dyes by textile effluent non-adapted and adapted aeromonas hydrophila. Environ Res 194:110643. https://doi.org/10.1016/j.envres.2020.110643

Fu S, Li P, Huang J, Meijuan G, Liu Z, Yanhua X (2021) Photocatalytic degradation of organic dye and tetracycline by ternary Ag_2O/AgBr–CeO_2 photocatalyst under visible-light irradiation. Sci Rep. https://doi.org/10.1038/s41598-020-76997-0

Zada N, Khan I, Shah T et al (2020a) Ag–Co oxides nanoparticles supported on carbon nanotubes as an effective catalyst for the photodegradation of Congo red dye in aqueous medium. Inorg Nano-Metal Chem. https://doi.org/10.1080/24701556.2020.1713159

Zada N, Saeed K, Khan I (2020b) Decolorization of rhodamine B dye by using multiwalled carbon nanotubes/Co–Ti oxides nanocomposite and Co–Ti oxides as photocatalysts. Appl Water Sci 10:40. https://doi.org/10.1007/s13201-019-1124-4